Observation of nitrogen vacancy photoluminescence from an optically levitated nanodiamond

Levi P. Neukirch,[1] Jan Gieseler,[2] Romain Quidant,[2,3] Lukas Novotny,[4,5] and A. Nick Vamivakas[5,*]

[1]*Department of Physics and Astronomy, University of Rochester, Rochester, New York 14627, USA*

[2]*ICFO-Institut de Ciencies Fotoniques, Mediterranean Technology Park, 08860 Castelldefels (Barcelona), Spain*

[3]*ICREA-Institució Catalana de Recerca i Estudis Avançats, 08010 Barcelona, Spain*

[4]*Photonics Laboratory, ETH Zürich, 8093 Zürich, Switzerland*

[5]*Institute of Optics, University of Rochester, Rochester, New York 14627, USA*

**Corresponding author: nick.vamivakas@rochester.edu*

Received May 8, 2013; revised June 26, 2013; accepted July 12, 2013;
posted July 12, 2013 (Doc. ID 190225); published August 6, 2013

We present what we believe to be the first evidence of nitrogen vacancy (NV) photoluminescence (PL) from a nanodiamond suspended in a free-space optical dipole trap at atmospheric pressure. The PL rates are shown to decrease with increasing trap laser power, but are inconsistent with a thermal quenching process. For a continuous-wave trap, the neutral charge state (NV^0) appears to be suppressed. Chopping the trap laser yields higher total count rates and results in a mixture of both NV^0 and the negative charge state (NV^-).

OCIS codes: (020.7010) Laser trapping; (160.0160) Materials; (160.2220) Defect-center materials; (160.2540) Fluorescent and luminescent materials; (350.4855) Optical tweezers or optical manipulation.
http://dx.doi.org/10.1364/OL.38.002976

The negatively charged nitrogen vacancy center (NV^-) in diamond has drawn substantial interest in quantum optics, quantum information [1,2], and nanoscale sensing [3–5]. It has proven to be a stable source of single photons [6], and displays a long ground-state spin coherence lifetime at room temperature [7]. It has served as a stable, optically accessible qubit in bulk diamond [8], and has been used to mediate spin reading and writing to ^{13}C nuclei [9]. Recently nanodiamonds containing ensembles of NV centers [10] and single defects [11] have been demonstrated to be well suited to biological magnetic sensing applications in optical tweezers and to sample characterization using microscopy techniques such as fluorescence lifetime imaging microscopy (FLIM) [12,13].

In this Letter we report the first measurement, to the best of our knowledge, of photoluminescence (PL) from a nanodiamond containing an ensemble of NV centers that is levitated in a free-space optical dipole trap. Such a system offers several advantages over previously demonstrated optical tweezer experiments. Most importantly, by eliminating the need for a liquid solution, our method represents a natural first step toward trapping nanodiamonds in vacuum, and implementing optomechanical cooling schemes [14,15]. Optically levitated and cooled dielectric particles have been demonstrated to be superb optomechanical resonators, with extremely high mechanical quality factors [16]. Furthermore, cooling the center-of-mass motion of these particles to their quantum ground state, while technically challenging, appears feasible [15]. Such a system using a nanodiamond containing an NV center, promises a hybrid quantum system of not only unprecedentedly high mechanical Q-factor, but one in which the Q-factor is tunable (via ambient pressure). A recent proposal suggests the possibility of generating Schrödinger cat states with an optically levitated nanodiamond [17].

The optical trap is formed by focusing a continuous wave neodynium:YAG laser (1064 nm) using a NA = 0.9 Nikon microscope objective (Fig. 1). An acousto-optic modulator (AOM) is positioned in the trap beam, with the first-order refracted beam used for trapping. The AOM is driven by a delay/pulse generator with subnanosecond precision (SRS DG535), allowing the trap laser to be chopped with rise/fall times of 100 ns (limited by the AOM response). The trap beam is then expanded to fill the back aperture of the trapping objective. A Picoquant LDH-FA pulsed laser (532 nm; 40 MHz, 100 ps pulsewidth) is used to excite the NV centers. PL is collected into a multimode fiber. A 537 nm long-pass filter positioned before the fiber prevents any excitation light from leaking into the fiber and exciting background fluorescence. A pair of long-pass dichroic beam splitters (edges at 560 and 776 nm) allows confocal alignment of all three optical channels. For these experiments, the fiber output passes though a 750 nm short-pass filter to remove any 1064 nm light before entering a 0.75 m long imaging spectrometer with a liquid-nitrogen-cooled CCD (Princeton Instruments).

Trapped particles are imaged from the side by focusing horizontally scattered laser light onto a CCD. To measure the motion of a trapped particle, an aspheric lens (NA = 0.68) is positioned after the trap to collimate the outgoing light. A beam sampler sends 10% of the outgoing light to monitor the particle's transverse-horizontal position using a D-mirror and balanced photoreceiver [18,19]. During position measurements the excitation laser is blocked before it reaches the chamber. These experiments were conducted at atmospheric pressure; however, to isolate the trap from air currents present in the laboratory, the trapping objective and collimating lens were housed in a cylindrical 8 in. diameter stainless steel chamber. The trapping optics were mounted in the chamber with off-the-shelf optomechanical components, and access for the laser beams and imaging was provided by optical-quality fused-silica windows.

We use commercially available fluorescent high-pressure high-temperature (HPHT) nanodiamonds manufactured by Adámas Nanotechnologies (ND-NV-100 nm).

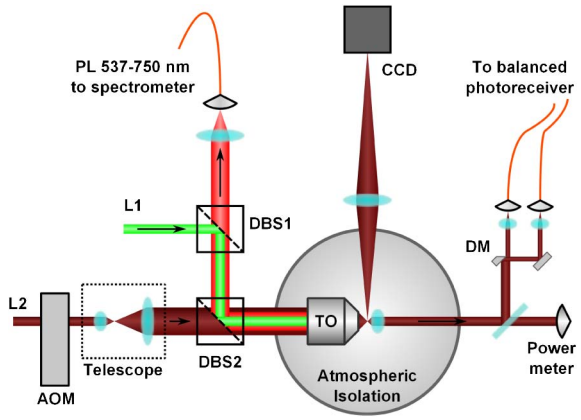

Fig. 1. Optical trap is formed in a vacuum chamber using the NA = 0.9 trap objective (TO). The excitation laser (L1) and PL are combined with a long-pass dichroic beam splitter (DBS1, 560 nm edge), and then combined with the trap laser (L2) using a second dichroic beam splitter (DBS2, 776 nm edge). The trap laser is chopped using an acousto-optic modulator (AOM) before being expanded by a lens pair.

The crystals are specified to have an average size of 100 nm and contain ~500 NV centers. The diamonds are used as shipped, with no subsequent processing to enhance their PL properties. To load the trap we mix a dilute solution (~1000:1) of the nanodiamond slurry with ethanol, and vaporize this solution with an ultrasonic nebulizer. The vapor is sprayed into the trapping chamber and we wait for diamonds to drift into the focal spot. This process typically results in a trapped particle after a few minutes.

Powers used for trapping (P_{trap}) usually range from 50 to 100 mW. Once trapped, most diamonds are stable in a CW or chopped trap for minutes to hours. An example of a typical position measurement is presented in Fig. 2(a). The output of the balanced photodetector is recorded via a computer (NI PCIe-6531 data acquisition card) or by a digital oscilloscope. At atmospheric pressure the harmonic nature of the trap is hidden by the high mechanical damping rate, and the motion is Brownian [20]. Power spectral densities of position show a high-frequency roll-off consistent with overdamped motion [see Fig. 2(b)]. Still, it is possible to estimate the size of a trapped particle.

By making the dipole and paraxial approximations, the displacements of a particle of mass m from trap center result in motion satisfying the Langevin equation [15,20],

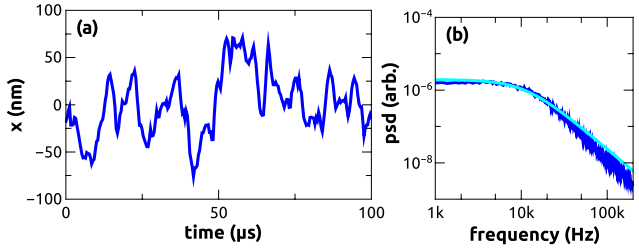

Fig. 2. At atmospheric pressure, (a) position measurements and (b) power spectra of position show the highly damped Brownian nature of the motion of an optically levitated nanodiamond. A curve fit to the PSD according to Eq. (2) is shown in cyan, and results in an estimated particle radius of 38 nm.

$$\ddot{x}(t) + \Gamma_0 \dot{x}(t) + \Omega_0^2 x(t) = \frac{1}{m} F_{\text{fluct}}(t). \tag{1}$$

Here Γ_0 is the mechanical damping caused by collisions with the surrounding gas, Ω_0 is the trap's natural frequency, and F_{fluct} is a random Langevin force satisfying $\langle F_{\text{fluct}}(t) F_{\text{fluct}}(t') \rangle = 2m\Gamma_0 k_B T \delta(t - t')$. The corresponding power spectral density (PSD) of this motion is described by

$$\text{PSD}(\omega) \propto \frac{\Gamma_0}{(\Omega_0^2 - \omega^2)^2 + \omega^2 \Gamma_0^2}. \tag{2}$$

For small displacements, the trap frequency is approximated by $\Omega_0 = \sqrt{k_{\text{trap}}/m}$, where k_{trap} is the trap stiffness. In the transverse direction [15]

$$k_{\text{trap}} = 4\pi^3 \frac{\alpha P}{c\varepsilon_0} \frac{(\text{NA})^4}{\lambda^4}, \tag{3}$$

depends on the optical system's NA, trapping power P, wavelength λ, and the particle's polarizability, α. For small spherical particles, $\alpha \propto R^3$. Thus the natural frequency,

$$\Omega_0 \propto \sqrt{\frac{R^3}{m}} \propto \sqrt{1/\rho}, \tag{4}$$

depends on density ρ, and is independent of particle size. We can therefore fit a measured PSD [cyan curve in Fig. 2(b)] using Eq. (2), while fixing Ω_0 according to Eq. (4). Determining Γ_0 from the fit allows us to estimate the particle radius, R, by using the Stokes friction coefficient, $\gamma = 6\pi\eta R$:

$$\Gamma_0 = \frac{\gamma}{m} = \frac{6\pi\eta R}{\rho\left(\frac{4}{3}\pi R^3\right)} = \frac{9\eta}{2\rho R^2}. \tag{5}$$

Here η is the dynamic viscosity of the surrounding medium. The data in Fig. 2(b) result in an estimated particle radius of 38 nm, which is within the tolerance quoted from the manufacturer.

PL spectra from a trapped nanodiamond are shown in Fig. 3(a). An average excitation power of 37 μW was used for all measurements, and an exposure time of 5 s was used to take each spectrum. Data are plotted for three different trapping powers. The spectra are readily identifiable as the characteristic 637 nm zero phonon line (ZPL) of the NV^- defect state, and broad phonon-assisted sidebands extending beyond 700 nm (truncated at 750 nm due to filtering). The spectra show an increase in PL rate across the entire phonon-assisted band as trapping power is decreased. Notably, we see no evidence for the NV^0 charge state when a continuous trap is used. Figure 3(b) shows the decrease in spectrally integrated count rate as a function of P_{trap}. Quenching of NV PL has been induced by heating samples to several hundreds of degrees Celsius [21,22]. The dependence displayed in Fig. 3(b), however, saturates at higher laser powers and is therefore inconsistent with heating due to absorption

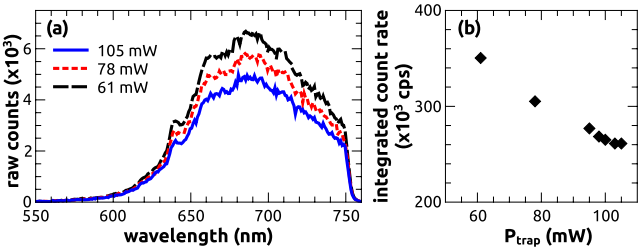

Fig. 3. (a) PL spectra show an increase when the trapping power is reduced, but little change in shape. (b) The spectrally integrated PL rate decreases with increasing trap laser power. Spectra and position measurements (Fig. 2) were measured on the same levitated nanodiamond.

of the trap beam. Rather, it is consistent with a recent study of two-color excitation of nanodiamonds containing single NV^- centers [23].

Given that reducing the power of the trap laser increases PL yield, we investigated the effect of chopping the trap beam (on the same nanodiamond). A constant trap-on power of 100 mW was used during chopping experiments. We used an AOM to chop the trap at a rate of 50 kHz (cycle period $T = 20$ μs), and varied the trap-off duration, Δt_{1064}, from 250 ns to 4 μs. Spectra for $\Delta t_{1064} = 0$, 2, and 4 μs are plotted in Fig. 4(a). The excitation power (37 μW) was the same as for the continuous trap experiment. We again measure spectra using 5 s exposures, and are thus averaging trap-on and trap-off PL. The spectra in Fig. 4(a) show higher count rates at all wavelengths when the trapping laser is chopped. A small peak at 575 nm (NV^0 ZPL) and elevated counts below 650 nm clearly indicate the emergence of the NV^0 state in the chopped-trap spectra. In Fig. 4(b) we plot the spectrally integrated counts for various values of Δt_{1064} (solid diamonds). The PL rates increase with the increase in trap-off time. To compare these with the data in Fig. 3(b), we compute average trap powers (top horizontal scale) by multiplying the trap-on power (100 mW) by the chopping duty cycle. We plot the integrated count rates from Fig. 3(b) for corresponding average trap powers (open diamonds). Chopping the trap beam results in a much more pronounced increase in integrated count rate than simply reducing the trap power.

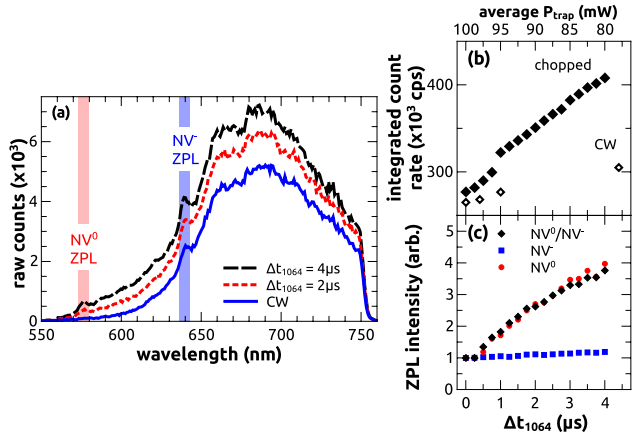

Fig. 4. (a) Chopping the trap laser at 50 kHz results in the emergence of the neutral (NV^0) charge state, as is evidenced by the ZPL at 575 nm, and increased counts at wavelengths shorter than 650 nm. As the trap-off duration, Δt_{1064}, increases, both (b) the total count rate and (c) the relative intensity of the NV^0 ZPL increase. The relative intensity of the NV^- ZPL appears to increase very slowly; however, this is likely due to a contribution from the rapidly increasing NV^0 sideband. Measurements were made on the same diamond as in Figs. 2 and 3.

In Fig. 4(c) we compare the relative changes in ZPL intensities. Plotted are the the heights of the NV^- ZPL (blue squares) and NV^0 ZPL (red dots) relative to the spectral peak (~690 nm), and the ratio of the intensities of the NV^0 ZPL to the NV^- ZPL (black diamonds). In each case, the data are normalized to their CW ($\Delta t_{1064} = 0$ ns) values. Clearly, the NV^0 ZPL is enhanced as the trap laser is modulated; however, it is not clear from these measurements whether this is due to a suppression of the NV^0 population, or simply a nonradiative quenching process that preferentially affects NV^0.

A number of authors have investigated NV photochromism using single color [24,25] excitation. Ivanov *et al.* [26] recently reported preferential NV^- excitation by two-photon absorption in the near infrared (1040 nm), and complete suppression of NV PL attributed to heating has been demonstrated under intense 1064 illumination [27]. To our knowledge, the suppression of NV^0 PL under simultaneous excitation by 532 nm and moderate 1064 nm illumination has not been previously reported. A more complete understanding of the mechanism underlying this suppression is important, given the significant implications for studies in which PL from the NV^0 state is undesirable.

In conclusion, we have, for the first time, demonstrated NV PL from a diamond levitated in a free-space optical trap. PL was excited by a 532 nm pulsed laser aligned confocally with the 1064 nm CW trap laser. PL rates are shown to increase as 1064 power decreases, and the nature of this dependence suggests the underlying cause is not thermally driven, indicating that heating is not a significant issue. We observe a high degree of suppression of PL from the NV^0 defect state while the trap laser is on. Chopping the trap laser on microsecond timescales increased the overall PL, and resulted in a mixing of PL from both the NV^0 and NV^- charge states.

The authors thank B. Deutsch and J. Cosentino for assistance with experiments, and three reviewers for their helpful comments. L. P. N. acknowledges support from the University of Rochester Department of Physics and Astronomy. A. N. V. acknowledges support from the Institute of Optics at the University of Rochester. Capital equipment available for this research was partially funded under Contract No. W911NF0910425 (N. George, PI) supported by Dr. Richard Hammond, Physics Division, U.S. Army Research Office. J. G. and R. Q. acknowledge support from the European Community's Seventh Framework Program under grant ERC-Plasmolight (no. 259196) and Fundació privada CELLEX. L.N. acknowledges support from the U.S. Department of Energy (Grant No. DE-FG02-01ER15204).

References

1. J. Wrachtrup and F. Jelezko, J. Phys. Condens. Matter **18**, S807 (2006).
2. P. Neumann, R. Kolesov, B. Naydenov, J. Beck, F. Rempp, M. Steiner, V. Jacques, G. Balasubramanian, M. L. Markham,

D. J. Twitchen, S. Pezzagna, J. Meijer, J. Twamley, F. Jelezko, and J. Wrachtrup, Nat. Phys. **6**, 249 (2010).
3. J. R. Maze, P. L. Stanwix, J. S. Hodges, S. Hong, J. M. Taylor, P. Cappellaro, L. Jiang, M. V. G. Dutt, E. Togan, A. S. Zibrov, A. Yacoby, R. L. Walsworth, and M. D. Lukin, Nature **455**, 644 (2008).
4. F. Dolde, H. Fedder, M. W. Doherty, T. Nöbauer, F. Rempp, G. Balasubramanian, T. Wolf, F. Reinhard, L. C. L. Hollenberg, F. Jelezko, and J. Wrachtrup, Nat. Phys. **7**, 459 (2011).
5. H. J. Mamin, M. Kim, M. H. Sherwood, C. T. Rettner, K. Ohno, D. D. Awschalom, and D. Rugar, Science **339**, 557 (2013).
6. C. Kurtsiefer, S. Mayer, P. Zarda, and H. Weinfurter, Phys. Rev. Lett. **85**, 290 (2000).
7. P. L. Stanwix, L. M. Pham, J. R. Maze, D. Le Sage, T. K. Yeung, P. Cappellaro, P. R. Hemmer, A. Yacoby, M. D. Lukin, and R. L. Walsworth, Phys. Rev. B **82**, 201201 (2010).
8. F. Jelezko, T. Gaebel, I. Popa, M. Domhan, A. Gruber, and J. Wrachtrup, Phys. Rev. Lett. **93**, 130501 (2004).
9. P. C. Maurer, G. Kucsko, C. Latta, L. Jiang, N. Y. Yao, S. D. Bennett, F. Pastawski, D. Hunger, N. Chisholm, M. Markham, D. J. Twitchen, J. I. Cirac, and M. D. Lukin, Science **336**, 1283 (2012).
10. V. R. Horowitz, B. J. Alemán, D. J. Christle, A. N. Cleland, and D. D. Awschalom, Proc. Natl. Acad. Sci. USA **109**, 13493 (2012).
11. M. Geiselmann, M. L. Juan, J. Renger, J. M. Say, L. J. Brown, F. J. G. de Abajo, F. Koppens, and R. Quidant, Nat. Nanotechnol. **8**, 175 (2013).
12. A. W. Schell, P. Engel, and O. Benson (2013), http://arxiv.org/abs/1303.0814.
13. R. Beams, D. Smith, T. W. Johnson, S. H. Oh, L. Novotny, and N. Vamivakas (2013), http://arxiv.org/abs/1303.1204.
14. T. Li, S. Kheifets, and M. G. Raizen, Nat. Phys. **7**, 527 (2011).
15. J. Gieseler, B. Deutsch, R. Quidant, and L. Novotny, Phys. Rev. Lett. **109**, 103603 (2012).
16. A. Ashkin and J. M. Dziedzic, Appl. Phys. Lett. **28**, 333 (1976).
17. Z. Yin, T. Li, X. Zhang, and L. M. Duan (2013), http://arxiv.org/abs/1305.1701.
18. F. Gittes and C. F. Schmidt, Opt. Lett. **23**, 7 (1998).
19. I. Chavez, R. Huang, K. Henderson, E. L. Florin, and M. G. Raizen, Rev. Sci. Instrum. **79**, 105104 (2008).
20. T. Li, S. Kheifets, D. Medellin, and M. G. Raizen, Science **328**, 1673 (2010).
21. T. Plakhotnik and D. Gruber, Phys. Chem. Chem. Phys. **12**, 9751 (2010).
22. D. M. Toyli, D. J. Christle, A. Alkauskas, B. B. Buckley, C. G. Van de Walle, and D. D. Awschalom, Phys. Rev. X **2**, 031001 (2012).
23. M. Geiselmann, R. Marty, J. F. García de Abajo, and R. Quidant, "Room temperature optical transistor based on a single nv centre in diamond," Nat. Phys. (to be published).
24. T. L. Wee, Y. K. Tzeng, C. C. Han, H. C. Chang, W. Fann, J. H. Hsu, K. M. Chen, and Y. C. Yu, J. Phys. Chem. A **111**, 9379 (2007).
25. N. Aslam, G. Waldherr, P. Neumann, F. Jelezko, and J. Wrachtrup, New J. Phys. **15**, 013064 (2013).
26. I. P. Ivanov, X. Li, P. R. Dolan, and M. Gu, Opt. Lett. **38**, 1358 (2013).
27. N. D. Lai, O. Faklaris, D. Zheng, V. Jacques, H. C. Chang, J. F. Roch, and F. Treussart (2013), http://arxiv.org/abs/1302.2154.